MediPharm

International Journal of MediPharm Research

ISSN:2395-423X www.medipharmsai.com

Vol.03, No.01, pp 178-186, 2017

Structural and antibacterial effect of $CaFe_XMn_{1-X}O_{3-\delta}$ & $BaFe_XMn_{1-X}O_{3-\delta}$ Perovskite films

M. Balaji[1]*, B. Lalitha Maheswari [1] and R.A. Jeyaram [2]

[1] Department of Physics, Sourashtra College, Madurai – 625 004, Tamil Nadu, India.
[2] Department of Physics, Senthamarai College of Arts and Science, Madurai – 625 021, Tamil Nadu, India.

Abstract : Some of the pervoskite materials are exhibits perfect antibacterial effect, so they are applied in surgical tool. Due to their non-toxic properties these perovskite coating materials may serve internal and external applications of human bodies. In this concern, here we report $CaFe_xMn_{1-x}O_{3-\delta}$ and $BaFe_xMn_{1-x}O_{3-\delta}$ (x = 0, 0.5 and 1) films on amorphous glass substrate synthesized by spin coating technique. The structural and morphological behaviour are identified by XRD and AFM analysis respectively. The crystallinity appeared only after annealing the films at 450°C. There is peak shifting takes place due to the addition of Fe^{3+} in Mn^{3+} ions. The existence of oxygen vacancy in complex elements is mainly due to the partial replacement of different elements on B-site, which strongly affects the oxygen vacancy. AFM analysis is taken under tapping mode, shows large numbers of spherical particles with the average particle size of 34 nm for $BaFe_{0.5}Mn_{0.5}O_{3-\delta}$. The antibacterial activity of $CaFe_{0.5}Mn_{0.5}O_{3-\delta}$ and $BaFe_{0.5}Mn_{0.5}O_{3-\delta}$ films are tested against two gram positive (*Staphylococcus Aureus* and *Klebsiella Pneumoniae*) and two gram negative (*Pseudomonas* and *Escherichia Coli*) bacteria. In which, $CaFe_{0.5}Mn_{0.5}O_{3-\delta}$ is active against *Pseudomonas* and $BaFe_{0.5}Mn_{0.5}O_{3-\delta}$film is active against *Staphylococcus Aureus* bacteria and their zone of inhibition is 23 mm and 18 mm respectively.
Keywords: X-ray diffraction; Atomic Force Microscopy; Perovskite Film; Antibacterial Effect.

1. Introduction

Perovskite films have recently been studied in great detail because of their interesting application in biomedical field [1]. However there is no report about the antibacterial effect of the films. Hence there is a need for the development of broad-spectrum antimicrobial coatings that are active against potentially pathogenic bacteria and hence this study is carried out.

The growth of the films by a simple and economic deposition technique has been playing an important role in the surgical field, in order to reduce the device fabrication cost. In this report, we have outlined the simple and economic technique as Sol-Gel spin coating technique method to fabricate a perovskite film. Also an attempt has been made to study the antibacterial activity against the test organisms for the perovskite films.

The perovskite compound is $ABX_{3-\delta}$, where 'A' and 'B' are two cations of very different sizes and X is an anion that bonds to both. The 'A' atoms are larger than the 'B' atoms. The most common perovskite compounds contain oxygen; there are a few compounds that form without oxygen ($NaMgF_3$). C.Callender and D.P.Norton explained that the $BaFeO_3$ thin films grown between 650 ° and 850 °C yield of oxygen deficient that decreases in lattice spacing with increasing growth temperature [2]. $CaMnO_3$ has high electrical

conductivity, electro catalytic activity and stability [3]. Recently, the occurrence of antibacterial activity on perovskite materials, such as $Ag_{0.3}Na_{1.7}La_2Ti_3O_{10}$ is reported against *E.Coli* and *S.aureus*, while its discoloration was not observed after 24 hrs light ageing test [4].

The film coating is used on a variety of medical devices, including orthopaedic implants, pacemakers, surgical instruments, orthodontic appliances and dental instruments. The organic compounds traditionally used for disinfection pose several disadvantages, including toxicity to the human body and sensitivity to high temperatures and pressures that are present in many industrial processes [5]. For these reasons, the interest in inorganic disinfectants such as metal oxides are increasing [5,6]. These inorganic compounds have strong antibacterial activity at low concentrations [7]. They are also much more stable in extreme conditions [8].

The plasma membrane or bacterial cytoplasmic membrane is composed of a phospholipid bilayer and thus has all of the general functions of a cell membrane such as acting as a permeability barrier for most molecules and serving as the location for the transport of molecules into the cell. In addition to these functions, prokaryotic membranes also function in energy conservation as the location about which a proton motive force is generated [9].

The most obvious structural characteristic of bacteria is (with some exceptions) their small size. For example, *Escherichia coli* cells have an average size 2 μm long and 0.5 μm in diameter, with a cell volume of 0.6 - 0.7 μm^3[10]. This corresponds to a wet mass of about 1 picogram, assuming that the cell consist mostly of water. The dry mass of a single cell can be estimated as 20% of the wet mass, amounting to 0.2 pg. About half of the dry mass of a bacterial cell consists of carbon, and also about half of it can be attributed to proteins. Therefore, a typical fully grown 1-liter culture of *Escherichia coli* yields about 1 g wet cell mass [9].

2. Experimental procedure

When referring to the synthesis method it is necessary to specify that, there are different methods available, each one has both advantages and disadvantages. In this study sol-gel spin coating technique is used to prepare the films, which is low cost and sol has been made at room temperature.

2.1. Materials

All the chemicals used in this experiment are purchased from E-Merck (Analytical Grade). The chemicals used for the preparation of films and functionalization of $CaFe_XMn_{1-X}O_{3-\delta}$ and $BaFe_XMn_{1-X}O_{3-\delta}$are $CaCl_2.2H_2O$, $BaCl_2.2H_2O$, $FeCl_3$ anhydrous, $MnCl_2.6H_2O$, Citric acid ($C_6H_8O_7$) and Diethylene Glycol (DEG). Throughout the experiment double distilled de-ionized water used.

2.2. Preparation of films

The $CaFe_XMn_{1-X}O_{3-\delta}$ and $BaFe_XMn_{1-X}O_{3-\delta}$ films (with x = 0, 0.5and 1) are prepared by the Sol-Gel technique. In order to obtain the sol, the desired stoichiometric proportion of the $CaCl_2.2H_2O$ and $FeCl_3$materials are weighted. The weighted samples, 0.06M of $C_6H_8O_7$ and 11.4 ml of DEG solution are added and keep under continuous stirring. Throughout the experiment the temperature is maintained at 50^oC. After the samples are fully dissolved in the solution, 15 ml ofH_2O is added. The final solution is stirred about 30 minutes to create a sol solution. After the solution is cooled down to the room temperature, the solution is applied on the amorphous glass plate to make layers. To make a homogenous film, the substrate is kept on our own spin coating unit. Initially, the spin coater is set at approximately 500 rpm value for 1 minute then, the speed of the coater will gradually increase up to 2500 rpm for 1 to 5 minutes. The coated samples are subsequently annealed at 450 ^oC in air for 0-3 hours.

2.3. Characterization techniques

The structural analysis of $CaFe_XMn_{1-X}O_{3-\delta}$ and $BaFe_XMn_{1-X}O_{3-\delta}$ films are carried out by PANalytical X'Pert Pro X-ray diffractometer using Cu-Kα radiation with step size of 0.05^o and the 2θ ranges from 10^o to 80^o. The surface morphology is studied by Atomic Force Microscopy (AFM) with silicon cantilever tip by tapping mode of resolution 2 μm. The antibacterial activity of $CaFe_{0.5}Mn_{0.5}O_{3-\delta}$ (CFMO) and $BaFe_{0.5}Mn_{0.5}O_{3-\delta}$ (BFMO) films are screened by Disc diffusion method.

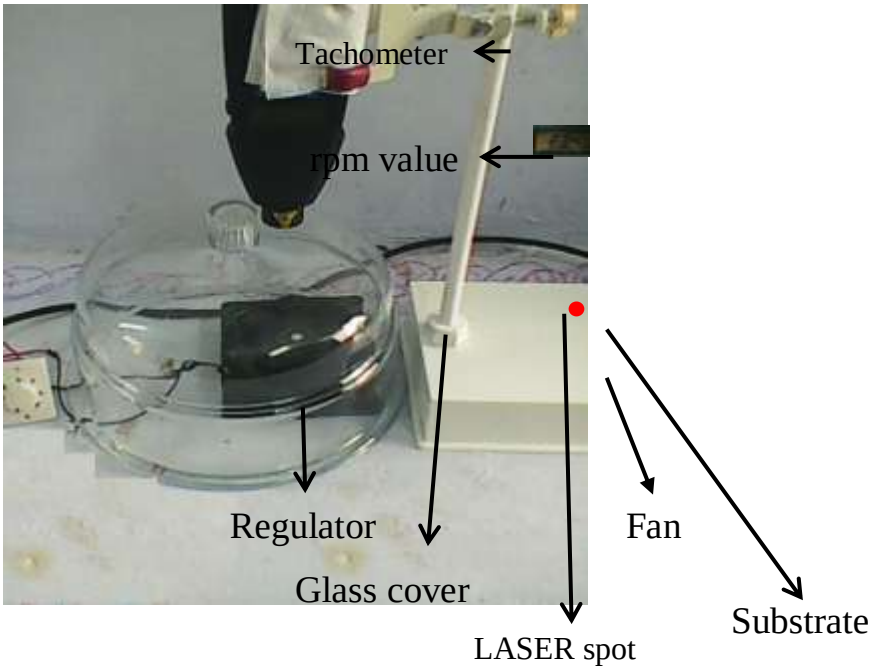

Figure 1. Lab Made Spin Coater

2.4. Antibacterial Analysis

Antibacterial activity is screened by Disc diffusion – Kirby Bauer method with Muller Hinton Agar (MHA) plates. The MHA plates are prepared by pouring 25 ml of molten media into sterile petri plates and allowed to solidify. *Staphylococcus aureus, Klebsiella Pneumoniae, Escherichia coli* and *Pseudomonas* are used for the study of antimicrobial test.

The prepared MHA plates are swabbed with the 0.1% inoculums suspension of 24 hrs broth culture and allow to dry for 5 mins. The films with different samples are placed on the surface of medium and the plates are kept for incubation for 24 hrs at 37 $^{\circ}$C. Before that, the coated films are cut manually as 1x1 cm^2 area by glass cutter with diamond pointer. Nalidixic acid is used as positive and controls respectively. At the end of the incubation, zone of inhibition is formed around the disc are measured.

3. Results and discussion

XRD studies are performed for all the films prepared are represented by the Fig.2 and Fig.3 According to the result (Fig. 2), there are three important peaks (011), (002) and (243) are appeared in the films, which are confirmed by the JCPDS file # 03-0804 for $CaFeO_{3-\delta}$ (CFO) and # 03-0830 for $CaMnO_{3-\delta}$ (CMO). In addition to that a broad hump ranges from 20° to 30° are also appeared for glass substrate [11]. The CFO and CMO film has the structure of orthorhombic and cubic symmetry respectively, which is confirmed by JCPDS files.

From Fig.2a, Fe ion doping induces stronger and sharper peak. In CMO film (Fig.2b) the 2θ of 69.72^{o} peak is shifted to 67.54^{o} in (Fig.2a). This shifting is due to the substitution of Fe^{3+} cations instead of Mn^{3+} cations [12]. The combination of (243) peak in CFO film and the peak at 2θ of 69.72° in CMO film produce the combined peak at 62.04° in CFMO film.

The crystallinity of CFO film is observed high, which is understood by the 100% intensity of the peak 31.77^{o} with d-spacing of 2.81 from the plane (002).

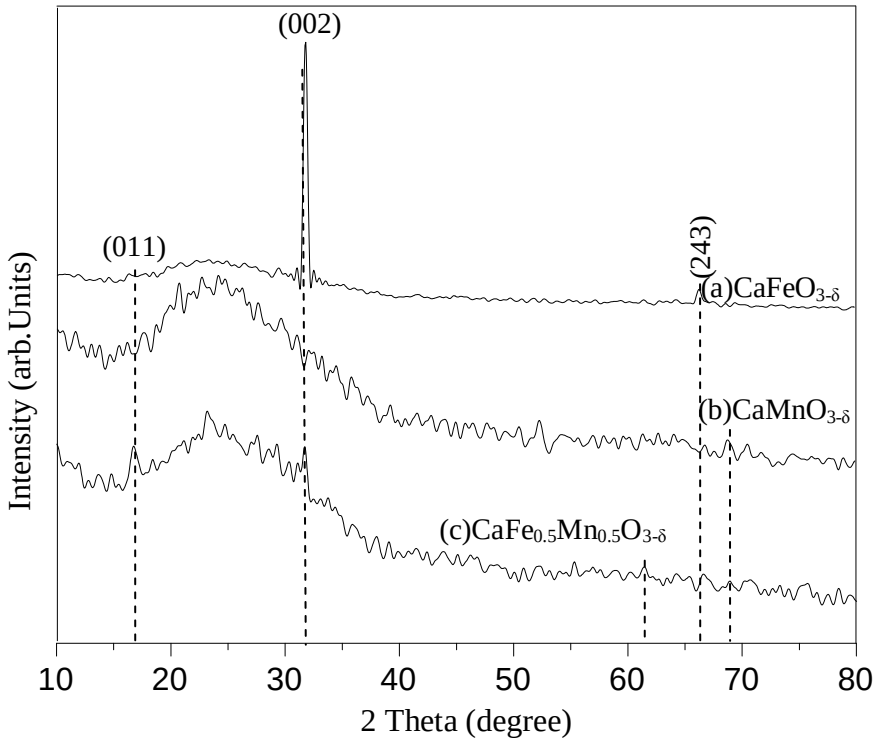

Figure 2. XRD Pattern of $CaFe_XMn_{1-X}O_{3-\delta}$ films (X=0, 0.5, 1)

In general, structure of A-site and B-site elements measuring the stoichiometric ratio of oxygen [13, 14]. Here the partial replacement of B-site strongly affects the redox properties of Fe ions and the stability of oxygen vacancy.

Figure.3, shows that, the stronger diffraction pattern of the substrate and weaker diffractions of the films. From (Fig.3a) $BaFeO_{3-\delta}$ (BFO) film peaks are obtained in the hkl plane value of (102), (061) and (054) and depicts the orthorhombic structure. The weaker diffractions are found, which may be due to minimum thickness of the film. If the thickness of the film increases, the reflection peak intensity may be increased.

The peaks corresponds to the two theta of 33.95^o from (Fig.3a), and the peak correspond to 28.769^o from (Fig.3b) are merged in (Fig.3c), due to the composition of iron and manganese ions. The $BaMnO_{3-\delta}$ (BMO) film is in hexagonal structure.

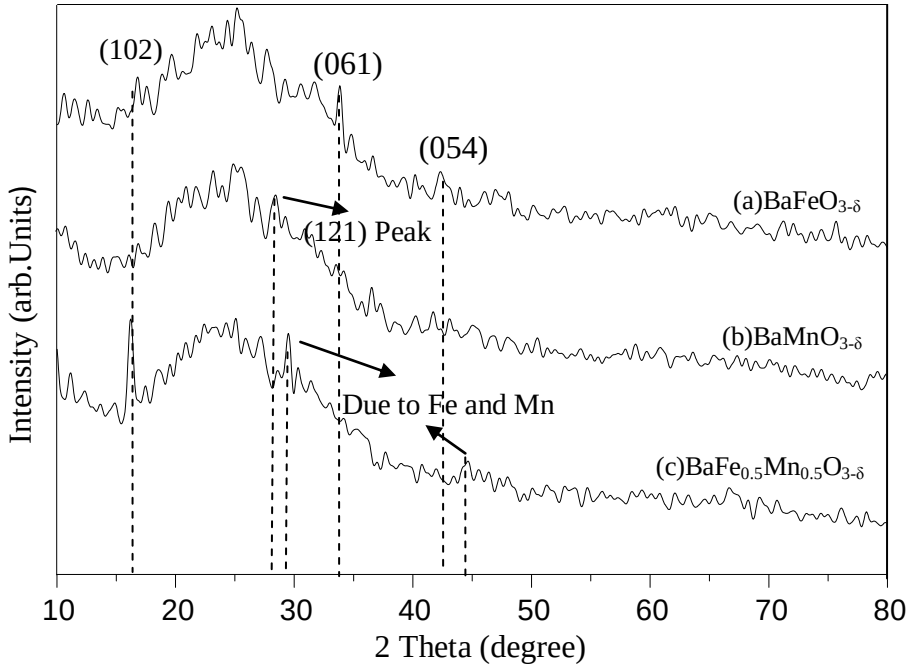

Figure 3. XRD pattern of $BaFe_XMn_{1-X}O_{3-\delta}$ films (X=0, 0.5, 1)

From Fig 3, most prominent peaks are (102), (061) and (054) observed in BFO film, the peak (102) is also present in BFMO film with high intensity, this is clear that the Mn ions is partially substituted with Fe ions. The (121) peak is presented in the BMO film. The combination of planes (121) in (Fig.3b) and (061) in (Fig.3a) are produce the combined peak in 29.65^o in (Fig.3c). In BFO film (061) peak is shifted to the lower angle and (121) peak is shifted to greater two theta angle.

The comparison of average crystallite size, cell parameters and strain of the $CaFe_XMn_{1-X}O_{3-\delta}$ and $BaFe_XMn_{1-X}O_{3-\delta}$ films are tabulated in Table.1. From CFO and CMO, lattice parameter value of (a) increased by increasing the Mn concentration. [15]

The appearance of low intensity diffraction peaks on CFMO and BFMO films are mainly due to the thickness and annealing effect of the films [16, 17]. Size broadening due to the crystallite size distribution is found by the formula, $D = {k\lambda}/{\beta \cos\theta}$. Where, D is the crystallite size, β is the FWHM of the observed peak, λ is the wavelength of the X-Ray diffraction, k is the dimensionless shape factor and θ is the angle of diffraction. Broadening due to strain in the sample can be calculated using the formula $\epsilon = {\beta}/{4\tan\theta}$. β is the FWHM of the observed peak and θ is the angle of diffraction [18].

Table 1.Comparison of cell parameter, average crystallite size (D) and strain (ϵ)

Sample	**JCPDS Value**			**Average** Crystallite size (D) X 10^{-9}m	**Average** Strain (ϵ) X 10^{-3}
	Cell Parameter				
	a (Å)	b (Å)	c (Å)		
$CaFeO_{3-\delta}$(CFO)	5.42	14.75	5.59	68	5.30
$CaMnO_{3-\delta}$(CMO)	7.46	-	-	66	2.97
$CaFe_{0.5}Mn_{0.5}O_{3-\delta}$(CFMO)	-	-	-	89	2.51
$BaFeO_{3-\delta}$(BFO)	5.92	16.46	11.01	57	2.96

$BaMnO_{3-\delta}$(BMO)	5.70	-	4.82	63	2.97
$BaFe_{0.5}Mn_{0.5}O_{3-\delta}$(BFMO)	-	-	-	83	3.22

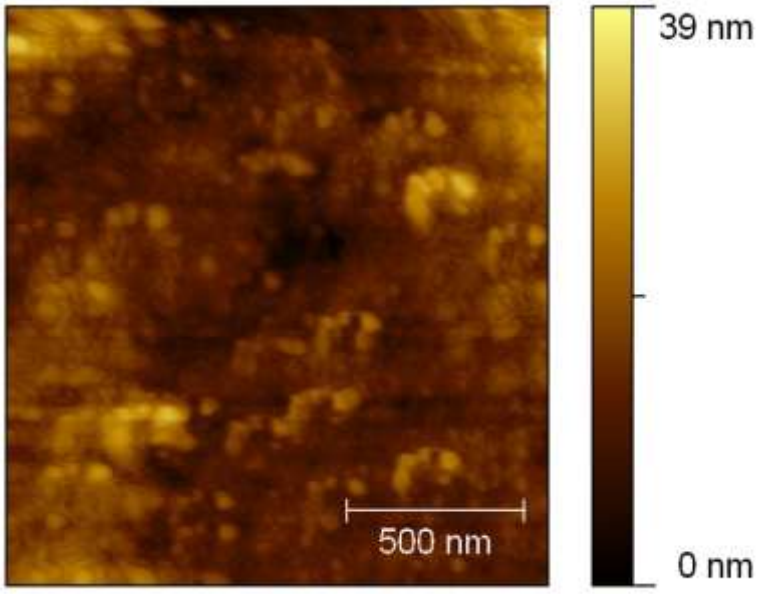

Fig. 4. AFM image of $BaFe_{0.5}Mn_{0.5}O_{3-\delta}$

In $BaFe_{0.5}Mn_{0.5}O_{3-\delta}$ film, Fig.4, image shows the presence of fine blocks of elements, where the spherical particles are embedded on the substrate of the film are found by tapping mode with non-contact cantilever tip. The average particle size of$BaFe_{0.5}Mn_{0.5}O_{3-\delta}$ is 34 nm, which clearly attributes the particles are in nano range. In $CaFe_{0.5}Mn_{0.5}O_{3-\delta}$ film, the surface is very smooth; we cannot obtain the AFM image even change the height of the cantilever tip.

In tapping mode, AFM cantilever is oscillating close to its resonance frequency. An electronic feedback loop ensures that the oscillation amplitude remains constant, such that a constant tip-sample interaction is maintained during scanning. Forces that act between the sample and the tip will not only cause a change in the oscillation amplitude, but also change in the resonant frequency and phase of the cantilever [19].

In the study of two films, $BaFe_{0.5}Mn_{0.5}O_{3-\delta}$ had high Van der waals force between the Ba, Fe and Mn atoms. But, $CaFe_{0.5}Mn_{0.5}O_{3-\delta}$ film, the long-range force is very small, due to the concentration of the elements present in the films. The Van der waals force between the cantilever and film surface is very small. So, AFM cannot measure the value.

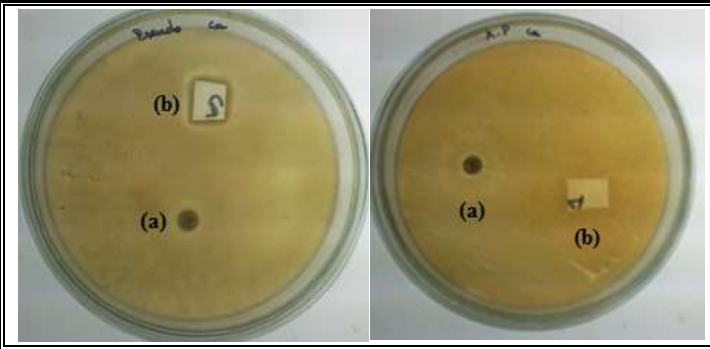

Pseudomonas *Klebsiella Pneumoniae*

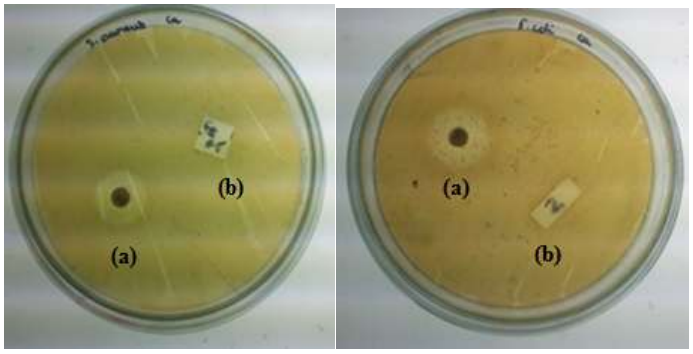

Staphylococcus aureus *Escherichia coli*

Figure.5(i). Anti bacterial activity of $CaFe_{0.5}Mn_{0.5}O_{3-\delta}$, where (a)Reference; (b) Film sample

From Figure.5 (i) and (ii), the antibacterial activity of $BaFe_{0.5}Mn_{0.5}O_{3-\delta}$film is only active against *Staphylococcus aureus* bacteria and $CaFe_{0.5}Mn_{0.5}O_{3-\delta}$ film is active only for *Pseudomonas* bacteria. It is not active in other three bacteria's. It may be due to insufficient amount of the material used or the material could not pass through the cell wall of bacteria's.

The polarity of cell membrane also affects the materials, not to pass into the bacteria. Sonohara et al. [20] have reported that the *S. aureus* membrane has a smaller negative charge. This would allow a higher level of penetration of negatively charged free radicals such as superoxide radical anions and peroxide ions, (Fe^{3+} and Mn^{3+}), causing damage and cell death to *S. aureus* at lower concentrations.

For other bacteria, the cell membrane is not diffused by the ions, such as Fe and Mn in the ratio of 0.5:0.5. If the concentration increases cell membrane may be easily diffused. The cell wall of gram positive bacteria is thick, which is made up of Peptidoglycan layer as 95%, which mainly contains negatively charged groups such as carboxyl, amide and hydroxyl groups. Gram negative cell walls are thin; it contains a thin layer of Peptidoglycan. The $CaFe_XMn_{1-X}O_{3-\delta}$ and $BaFe_XMn_{1-X}O_{3-\delta}$ film contains cations as Ca or Ba, Fe^{3+} and Mn^{3+}.

The cell wall diffusion is carried out by a physicochemical mechanism and it depends mainly on the active binding site of the metal ions with the micro-organisms. The metal binds onto the cell surface probably electrostatic interactions, Van-der Waals force and covalent bonding. The cell wall of bacteria is abundantly available with negatively charged groups, which will actively bind with the cations such as Ca^{2+} or Ba^{2+}, Fe^{3+} and Mn^{3+} [21]. The amount of anion is very less when compared to the cations present in the $CaFe_XMn_{1-X}O_{3-\delta}$ and $BaFe_XMn_{1-X}O_{3-\delta}$ films. The role of positive ions present in the film helps in promoting cell growth as well as preventing extensive cell wall damage and possible cell analysis [22].

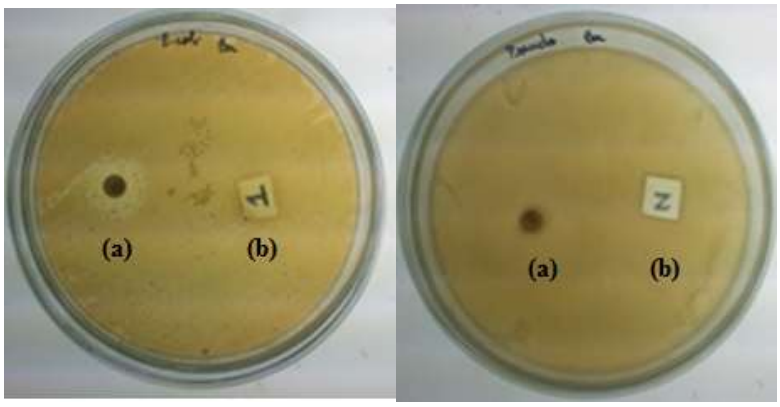

Escherichia coli *Pseudomonas*

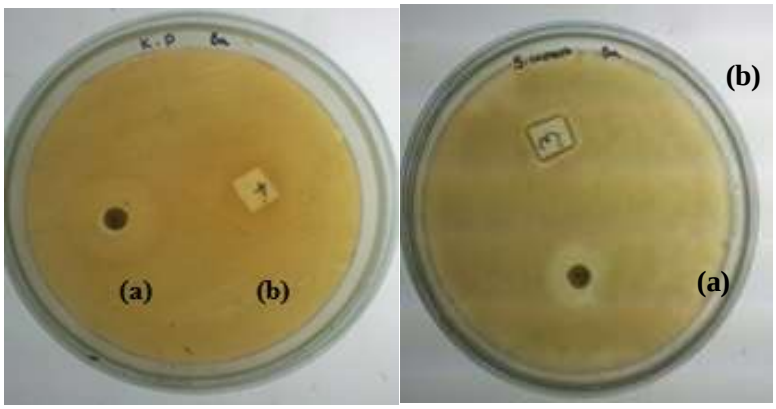

Klebsiella Pneumoniae *Staphylococcus aureus*

Figure.5(ii). Antibacterial activity of $CaFe_{0.5}Mn_{0.5}O_{3-\delta}$ Where (a)Reference; (b) Film sample

4. Conclusion

$CaFe_XMn_{1-X}O_{3-\delta}$ and $BaFe_XMn_{1-X}O_{3-\delta}$ films (where x = 0, 0.5, 1.0) are prepared by Sol-Gel spin coating technique; the lab-made spin coater is used to coat the films on the amorphous glass substrate. Coated films are annealed at 450 ^{0}C for 3 hrs to get the homogenous crystalline surface. The crystallinity of CFO film is high, due to the Fe^{3+} ions. The addition of Fe concentration peaks are getting strong and sharper. The average crystallite size is in the range of 43 to 86 nm. Several weak peaks are observed in $BaFe_xMn_{1-x}O_{3-\delta}$ film, which is mainly due to the thickness of the film. In which, the peak of BFO film at 33.95° and BMO peak at 28.77° are combined in the BFMO film. The range of crystallite size of the $BaFe_xMn_{1-x}O_{3-\delta}$ film is 20 nm to 56 nm. The antibacterial activity of CFMO and BFMO films are studied for two gram positive *Staphylococcus auerus and Klepciella pneumonia* bacteria and two gram negative *Escherichia coli and Pseudomonas* bacteria by Disc diffusion – Kirby Bauer method. The activity of films studied after 24 hours, CFMO and BFMO films are active against *Pseudomonas* and *Staphylococcus auerus* bacteria respectively. Their respective zone of inhibition is 23 mm and 18 mm. The surface of BFMO film is studied by Atomic Force Microscope. There are fine spherical particles are embedded on the surface of the film. The calculated average particles size is about 34 nm.

References

1. Simona Liliana Iconaru, Patrick Chapon, Philippe Le Coustumer and Daniela Predoi. Antibacterial activity of thin solid films of Silver doped Hydroxyapatite prepared by sol-gel method. The ScientificWorld Journal 2014; 165351: 1-8.
2. Callender C, Norton DP, Das R, Hebard AF and Budai JD. Ferromagnetism in pseudocubic $BaFeO_3$ epitaxial films. Appl. Phys. Lett. 2008; 92(1): 012514-1.
3. Coey JMD, Viret M, Von Molnar S. Mixed valence manganites. Advances in physics 1999; 48(2): 167-293.
4. Shao Zao Tan, Liu Cai Ding, Ying Liang Liu, You Sheng Ouyang, Yi Ben Chen. Synthesis and antibacterial activity of new layered perovskite compounds, $Ag_xNa_{2-x}La_2Ti_3O_{10}$. Chinese Chemical Letters 2007; 18(1): 85-88.
5. Yamamoto O. Influence of particle size on the antibacterial activity of zinc oxide. International Journal of Inorganic Materials 2001; 3: 643–646.
6. Zhang L, Jiang Y, Ding Y, Povey M, York D. Investigation into the antibacterial behaviour of suspensions of ZnO nanoparticles (ZnO nanofluids). Journal of Nanoparticle Research 2007; 9: 479–489.
7. Yiheyis Bogale Zemede, Nithyakalyani D and Ananda Kumar S. Synthesis, Characterization, Antimicrobial and Corrosion Inhibition Evaluation of Onno-Chelating Schiff Base Ligand and its Metal Complexes, International Journal of MediPharm Research, 2016, 2 (2), 128-141.
8. Sawai J. Quantitative evaluation of antibacterial activities of metallic oxide powders (ZnO, MgO and CaO) by conductimetric assay. Journal of Microbiological Methods 2003; 54: 177–182.
9. Capaldo-Kimball F. Involvement of Recombination Genes in Growth and Viability of Escherichia coli K-12. J. Bacteriol. 1971; 106(1): 204–212.
10. Kubitschek HE. Cell volume increase in Escherichia coli after shifts to richer media. J. Bacteriol.1990; 172 (1): 94–101.
11. Thiruramanathan P, Hikku GS, Krishna Sharma R and Siva Shakthi M. Preparation and characterization of indium doped SnS thin films for solar cell applications, International Journal of TechnoChem Research, 2015, 1 (1), 59-65.
12. Yongjin Luo, Xiuyun Wang, Qingrong Qian, Qinghua ChenStudies on B sites in Fe-doped $LaNiO_3$ perovskite for SCR of NO_x with H_2. International journal of hydrogen energy 2014; 39: 15836-15843m.
13. Oishi M, Yashiro K, Hong J, Nigara Y, Kawada T, Mizusaki J. Oxygen non-stoichiometry of B-site doped $LaCrO_3$. Solid State Ionics 2007; 178(3-4): 307-312.
14. Onuma S, Yashiro K, Miyoshi S, Kaimai A, Matsumoto H, Nigara Y, Kawada T, Mizusaki J, Kawamura K, Sakai N, Yokokawa H. Oxygen nonstoichiometry of the perovskite-type oxide $La_{1-x}Ca_xCrO_{3-\delta}$ (x=0.1, 0.2, 0.3). Solid State Ionics 2004; 174(1-4): 287-293.
15. Mandal P, Serrao CR, Suard E, Caignaert V, Raveau B, Sundaresan A and Rao CNR. Spin reorientation and magnetization reversal in the perovskite oxides, $YFe_{1-x}Mn_xO_3$ ($0 \leq x \leq 0.45$): A neutron diffraction study. Journal of Solid State Chemistry 2013; 197: 408–413.
16. Candeia RA, Bernardi MIB, Longo E, Santos IMG, Souza AG. Synthesis and characterization of spinel pigment $CaFe_2O_4$ obtained by the polymeric precursor method. Materials Letters 2004; 58(5): 569–572.
17. Shen CM, Zhang XG, Li HL. Influence of different deposition potentials on morphology and structure of CdSe films. Applied surface science 2005; 240(1-4): 34-41.
18. Bari RH, Selectivity of organic vapour for nanostructured CdO thin films prepared by sol-gel dip coating technique, International Journal of Chemical Concepts, 2015, 1 (3), 136-148.
19. Barrett S, Massalski TB. Structure of metals. McGraw-Hill, New York, (1966).
20. Sonohara R, Muramatsu N, Ohshima H, Kondo T. Difference in surface properties between Escherichia coli and Staphylococcus aureus as revealed by electrophoretic mobility measurements. Biophysical Chemistry 1995; 55: 273–277.
21. Yamazoe N and Teraoka Y. Oxidation catalysis of perovskites --- relationships to bulk structure and composition (valency, defect, etc.). Catal. Today 1990; 8(2): 175-199.
22. Doshi R, Alcock CB, Gunasekaran N and Carberry JJ. Carbon Monoxide and Methane Oxidation Properties of Oxide Solid Solution Catalysts. J. Catal. 1993; 140(2): 557-563.

*****